

# Deployment and Trajectory Optimization of UAVs: A Quantization Theory Approach

Erdem Koyuncu, Maryam Shabanighazikelayeh, and Hulya Seferoglu

## Abstract

Optimal deployment and movement of multiple unmanned aerial vehicles (UAVs) is studied. The considered scenario consists of several ground terminals (GTs) communicating with the UAVs using variable transmission power and fixed data rate. First, the static case of a fixed geographical GT density is analyzed. Using high resolution quantization theory, the corresponding best achievable performance (measured in terms of the average GT transmission power) is determined in the asymptotic regime of a large number of UAVs. Next, the dynamic case where the GT density is allowed to vary periodically through time is considered. For one-dimensional networks, an accurate formula for the total amount of UAV movement that guarantees the best time-averaged performance is determined. In general, the tradeoff between the total UAV movement and the achievable performance is obtained through a Lagrangian approach. A corresponding trajectory optimization algorithm is introduced and shown to guarantee a convergent Lagrangian. Numerical simulations confirm the analytical findings. Extensions to variable-rate fixed-power systems are also discussed.

## Index Terms

Unmanned aerial vehicles (UAVs), node placement, trajectory optimization, quantization theory.

## I. INTRODUCTION

Unmanned aerial vehicles (UAVs) can be effectively utilized in a variety of wireless communication scenarios. Example applications include providing coverage to geographical areas lacking

The authors are with the Department of Electrical and Computer Engineering, University of Illinois at Chicago. Emails: {ekoyuncu, mshaba7, hulya}@uic.edu

This work will be presented in part at the IEEE Wireless Communications and Networking Conference in April 2018 [1].

a wireless infrastructure, relaying to overcome terrain obstacles such as mountains, improving cell edge performance by creating femtocells, among many others [2]–[4].

One of the most distinguishing features of UAV networks is the opportunity of very fast dynamic adaptation to the ever-changing environment through relocation. Environmental variations in this context may include ground terminal (GT) location/density variations, UAV node failures, etc. Although the ability of relocation potentially offers significant performance gains, including improved coverage and rate for GTs, it also comes with many theoretical and practical challenges. Even in a static scenario where the locations or the density of GTs are known and fixed, finding the optimal UAV locations is a non-convex optimization problem whose dimensionality grows with the number of UAVs [2]. Dynamic scenarios further involve optimization of UAV trajectories, thus leading to much more complicated infinite-dimensional optimization problems.

Several approaches to resolve the challenges of UAV deployment/relocation have been proposed. In the case of static deployment, [5]–[7] consider the optimal placement of UAVs to maximize coverage and propose several algorithms. These works assume that a UAV can cover a GT provided that they are separated no more than a certain distance. In [8], the authors consider instead the average throughput as the objective function, and incorporate possible hover time constraints of UAVs into the problem formulation. Static placement of UAVs as relays for offloading cellular traffic [9], or generic multihop communication [10] have also been studied. Random deployments of UAVs are analyzed in [11] using tools from stochastic geometry.

There are also numerous works on dynamic deployment of UAVs. One well-studied scenario is to view UAVs as mobile access points serving GTs. For such a use case, algorithms for UAV coverage under variable coverage radii and possible UAV losses are proposed in [12]. For one UAV and one GT, [13] optimizes the UAV trajectory to achieve high throughput with low UAV energy consumption. A genetic algorithm for UAV trajectory optimization has been proposed in [14] with the specific goal of restoring network service after natural disasters. In [15], the authors optimize the trajectory of a single UAV serving multiple mobile GTs via space-division multiple access. A Kalman filter predicts the future GT locations, which, in turn, determine the UAV trajectory. Given several sensors on a one-dimensional space and one UAV, [16] determines

the time-varying UAV speed that minimizes the data collection time. A related problem is to optimize the UAV trajectories subject to speed constraints [17], [18]. In [19], the authors consider a UAV multicasting network-coded information to several GTs and the corresponding trajectory optimization problem. An algorithm to minimize the energy consumption of moving the UAVs from one deployment to another can be found in [20].

Several other works have considered the dynamic deployment problem in the context of UAVs serving as communication relays. In particular, for a single source-destination pair and one UAV, [21] develops a mobile UAV relaying method. The goal is throughput maximization via jointly optimizing UAV trajectory and temporal power allocation. The utilization of UAVs as relays between GTs and a central base station has been studied in [22], and a joint heading and adaptive handoff algorithm is proposed. In [23], [24], the authors design trajectory optimization algorithms for amplify-and-forward UAVs. For the case of one UAV and a circular trajectory, [25] optimizes the speed and load factor of the UAV for maximum energy efficiency. UAVs can also offer computation offloading opportunities in the context of edge computing. A corresponding trajectory optimization problem has been studied in [26] for the special case of a single UAV.

Despite many recent studies on UAV deployment and trajectory optimization, some of which have been described above, there are many fundamental open problems that are yet to be resolved. In particular, for static networks, there is no general analytical framework that can provide the optimal UAV positions for a given number of UAVs and spatial user density. Also, for the dynamic scenario, an analytical characterization of achievable performance gains are largely missing, and most of the above work relies on numerical methods for optimizing UAV trajectories and determining the resulting performance. Moreover, some of these trajectory optimization algorithms, including [13], [15], [21], [24]–[26], work only for one UAV, or one dimension [16]. Some, including [17]–[20], [22], [23], only consider UAV speed or instantaneous movement/energy limitations, and thus, do not incorporate a constraint on the long-term cost of mobility. Some other algorithms rely on methods such as simulated annealing [9] or genetic algorithms [14], and do not offer convergence guarantees or local optimality.

Quantization theory of data compression and source coding [27] has proved to be a very

successful analytical tool in addressing many existing problems that involve geographical deployment of agents [28]; examples applications of the theory include the deployment of antenna arrays [29], sensors [30], or general heterogeneous nodes [31]. The main contribution of this paper is to show that many of the aforementioned open problems on UAV networks can as well be formulated and ultimately resolved using a quantization theory approach. Our setup consists of a density of GTs that are served by an arbitrary number of UAVs. Each GT employs variable-power fixed-rate transmission to ensure outage-free reception at its closest UAV. In the static case, our goal is to find the optimal UAV deployment that minimizes the average GT transmission power, while in the dynamic case, we wish to minimize the time-averaged power consumption subject to the *total distance* traveled by the UAVs. The specific main contributions of this paper are then summarized as follows:

- In the static case, and a uniform distribution of GTs on a line segment on the ground, we determine the optimal deployment of UAVs and the resulting average GT power consumption. For a general one or two dimensional area on the ground and an arbitrary GT distribution, we determine the optimal deployment and the corresponding performance in the asymptotic regime of a large number of UAVs.
- In the dynamic case, for any dimension and any time-varying GT densities, we analytically characterize the optimal UAV deployments and the corresponding GT power consumptions in the two extremal cases of no UAV movement and unlimited UAV movement. In the special case of one dimension, our approach leads to an analytical formula for the total UAV movement that guarantees the lowest possible average GT power consumption.
- In order to address the case of moderate UAV movements, we introduce a trajectory optimization algorithm that relies on time discretization, and alternating optimization over each discretized time instance. The algorithm is a descent over the Lagrangian combination of GT power consumption and UAV movement. Optimization at each time instance is carried out through a generalization of Lloyd algorithm [32], [33] in vector quantization. Certain sub-optimization problems that arise in this context are solved in closed form.

Our algorithmic approach is thus more aligned with the Voronoi-based coverage control algorithms that were originally envisioned for mobile sensor networks [34]–[36]. These existing studies, however, do not consider total movement constraints and are thus not applicable.

Part of this work will be presented in a conference [1]. Compared to [1], most aspects of the trajectory optimization algorithm and the solutions to the accompanying sub-optimization problems are new. The current paper also provides more connections to the existing literature and more detailed numerical simulation results.

The rest of this paper is organized as follows: In Section II, we introduce the system model. We analyze static deployment of UAVs in Section III. We analyze the extremal cases of the dynamic deployment scenario in Section IV. In Section V, we introduce our trajectory optimization algorithm to address moderate movement constraints. We provide numerical simulation results in Section VI. Finally, in Section VII, we draw our main conclusions and discuss extensions to variable-rate transmission. Some of the technical proofs are provided in the appendices.

## II. SYSTEM MODEL

We consider a network of several GTs at zero elevation and several UAVs at a fixed elevation  $h > 0$ . Mathematically, we assume that the GTs are located on  $\mathbb{R}^d$ , where  $d \in \{1, 2\}$ . While typically one is interested in the case  $d = 2$ , i.e. when the GTs are in general positions on the ground, the case  $d = 1$  is also relevant: The GTs may be constrained to lie on a line on the ground, e.g. as cars on a straight highway.

We distinguish between what we refer to as the static and the dynamic deployment scenarios. In static deployment, we assume that the GTs are located on  $\mathbb{R}^d$  according to a certain fixed (time-invariant) density function  $f$ , where  $\int_{\mathbb{R}^d} f(q) dq = 1$ . In the more complicated dynamic deployment scenario, we will allow the user density to vary over time.

### A. Static Deployment

In order to formally describe the static deployment scenario, let  $x_1, \dots, x_n \in \mathbb{R}^d$  denote the UAVs' (projected) locations on the GT space. The squared Euclidean distance between a GT at

$q$  and the  $i$ th UAV at  $x_i$  is then given by  $\|x_i - q\|^2 + h^2$ . Fig. 1 provides an illustration for the special case of  $n = d = 2$ .

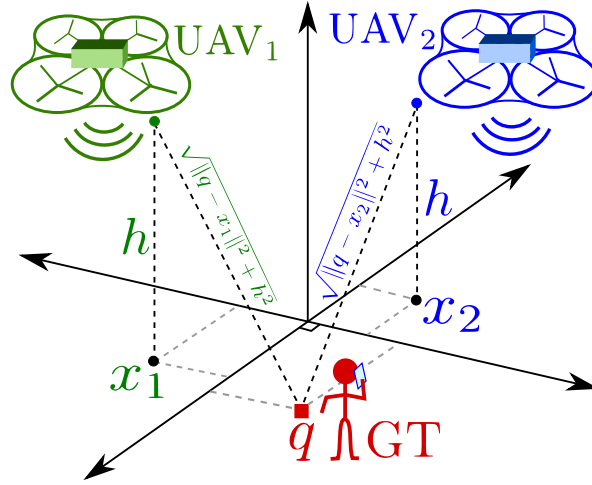


Fig. 1: A network of two UAVs serving a GT.

We first consider fixed-rate variable-power transmission at GTs. The case of fixed-power variable-rate transmission will be discussed later. Suppose that a GT at location  $q$  wishes to communicate with rate  $\rho$  bits/s/Hz, and transmits with power  $P$  J/s. From now on, we omit the units of all quantities for brevity. Due to the aerial nature of the communication system, we assume that there is line of sight between the GTs and the UAVs, and the effects of multipath fading is negligible. In such a scenario, the received signal power at a UAV at  $x_i$  is given by  $(\|x_i - q\|^2 + h^2)^{-\frac{r}{2}}P$ , where  $r$  is the path loss exponent. Reliable communication between the GT and the UAV is possible provided that the capacity of the (Gaussian) channel between the GT and the UAV is at least  $\rho$ , or, mathematically if  $\log_2(1 + (\|x_i - q\|^2 + h^2)^{-\frac{r}{2}}P) \geq \rho$ . The minimum transmission power of a GT at  $q$  that guarantees reliable data reception at a UAV at  $x_i$  is then  $\frac{2^\rho - 1}{P}(\|x_i - q\|^2 + h^2)^{\frac{r}{2}}$ . The minimum transmission power that guarantees successful data reception at at least one of the UAVs is therefore  $\min_i \frac{2^\rho - 1}{P}(\|x_i - q\|^2 + h^2)^{\frac{r}{2}}$ . Averaging out the user density, and setting  $\rho = P = 1$  without loss of generality, the average transmission power of GTs given UAV locations  $\mathbf{x} \triangleq [x_1 \cdots x_n]$  and GT density  $f$  is

$$P(\mathbf{x}, f) \triangleq \int_{\mathbb{R}^d} \min_i (\|x_i - q\|^2 + h^2)^{\frac{r}{2}} f(q) dq. \quad (1)$$

The static deployment problem is then to find the optimal UAV locations that minimize the average GT power consumption. In other words, we wish to determine  $P^*(f) \triangleq \min_{\mathbf{x}} P(\mathbf{x}, f)$ , and the optimal deployments  $\mathbf{x}^*$  that achieve  $P(\mathbf{x}^*, f) = P^*(f)$ .

### B. Dynamic Deployment

In practice, the GT density may vary over time. For example, in daily urban communications, the GT density over highways will be higher during rush hours, when compared to nighttime. In order to model such scenarios, we let  $f_t$  denote the GT density function at time  $t$ . We assume  $f_t$  is periodic over a time interval of length  $T$ , i.e.  $f_t(q) = f_{t+T}(q), \forall t, \forall q$ . For example, one may set  $T = 24$  hours for the urban communication scenario. We also assume that  $f_t(q)$  is continuous in both  $t$  and  $q$ . Thus, the GT density does not experience abrupt changes over space or time.

Let  $x_{i,t}$  denote the location of UAV  $i$  at time  $t$ , and  $\mathbf{x}_t = [x_{t,1} \cdots x_{t,n}]$  denote the vector of UAV locations at time  $t$ . The power consumption of GTs at time  $t$  is  $P(\mathbf{x}_t, f_t)$ . The average power consumption over time can be expressed as

$$Q \triangleq \frac{1}{T} \int_0^T P(\mathbf{x}_t, f_t) dt. \quad (2)$$

We have omitted to indicate the dependency of  $Q$  on  $\{(\mathbf{x}_t, f_t) : t \in [0, T]\}$  for brevity. The time-averaged distance traversed by the  $i$ th UAV can be calculated to be the line integral

$$M_i \triangleq \frac{1}{T} \int_0^T \sqrt{\sum_{j=1}^d \left| \frac{\partial x_{t,i,j}}{\partial t} \right|^2} dt, \quad (3)$$

where  $x_{t,i,j}$  represents the  $j$ th component of  $x_{t,i}$ . In this case, the goal is to find the optimal UAV trajectories that minimize the average GT power consumption  $Q$  subject to a constraint  $\sum_{i=1}^n M_i \leq M$  on the total UAV movement, where  $M \geq 0$  is given.

## III. OPTIMIZATION OF A STATIC DEPLOYMENT

We begin with the simpler scenario of a static deployment and its optimization. Namely, we study the minimization of (1) with respect to UAV locations  $\mathbf{x}$ . We begin by considering the degenerate case  $h = 0$ , in which case we can imagine that the network consists of unmanned ground vehicles (UGVs) instead of UAVs. The analysis of such a UGV scenario will be very useful for our analysis of the UAV case  $h > 0$ .

### A. The UGV Case $h = 0$

For  $h = 0$ , the cost function in (1) becomes

$$P(\mathbf{x}, f) = \int_{\mathbb{R}^d} \min_i \|x_i - q\|^r f(q) dq, \quad h = 0. \quad (4)$$

This expression is the well-known average  $r$ th power distortion of a quantizer whose reproduction points are  $x_1, \dots, x_n$  for a given source density  $f$ . Finding the exact minimizers of (4) and the corresponding minimum distortions is possible only for a few special cases. In particular, if  $f(q) = \mathbf{1}(q \in [0, 1])$  is the one-dimensional uniform density, then the optimal reproduction points are given by the uniform quantizer codebook  $\mathbf{x}_u = [\frac{1}{2n} \frac{3}{2n} \dots \frac{2n-1}{2n}]$  with  $P(\mathbf{x}_u, f) = \frac{1}{(1+r)(2n)^r}$ .

For a general uniform density, we have the following result of Bennett [37] and Zador [38]. Given  $A \subset \mathbb{R}^d$ , let  $m(A) \triangleq \int_A \|q\|^r dq / (\int_A dq)^{\frac{d+r}{d}}$  denote the normalized  $r$ th moment of  $A$ .

**Proposition 1.** *Let  $f(q) = \mathbf{1}(q \in [0, 1]^d)$ ,  $h = 0$ . As  $n \rightarrow \infty$ , we have  $P^*(f) = \kappa_{rd} n^{-\frac{r}{d}} + o(n^{-\frac{r}{d}})$ , where  $\kappa_{rd}$  depends only on  $r$  and  $d$ . In particular,  $\kappa_{r1} = \frac{2^{-r}}{1+r}$  and  $\kappa_{r2}$  are the normalized moments of the origin-centered interval and the origin-centered regular hexagon, respectively.*

This implies in particular that for two dimensions and a uniform distribution, the best arrangement of quantization points is asymptotically the regular hexagonal lattice.

Making the transition from uniform to non-uniform  $f$  can be accomplished using the idea of point density functions. In detail, one assumes the existence of a function  $\lambda(q)$  such that the cube  $[q, q + dq]$  of volume  $dq$  contains  $n\lambda(q)dq$  reproduction points with  $\int_{\mathbb{R}^d} \lambda(q)dq = 1$ . Since  $f$  should be approximately uniform on  $[q, q + dq]$ , the conditional average distortion on  $[q, q + dq]$  is  $\kappa_{rd}(n\lambda(q))^{-\frac{r}{d}} + o(n^{-\frac{r}{d}})$  by Proposition 1. Averaging out the density, we obtain the formula

$$\tilde{P}(\lambda) \triangleq \kappa_{rd} n^{-\frac{r}{d}} \int_{\mathbb{R}^d} f(q) \lambda^{-\frac{r}{d}}(q) dq + o(n^{-\frac{r}{d}}). \quad (5)$$

for the average distortion given  $\lambda$ . Using reverse Hölder's inequality, we have

$$\tilde{P}(\lambda) \geq \kappa_{rd} n^{-\frac{r}{d}} \|f\|_{\frac{d}{d+r}} + o(n^{-\frac{r}{d}}), \quad (6)$$

where  $\|f\|_{\alpha} \triangleq (\int_{\mathbb{R}^d} (f(q))^{\alpha} dq)^{\frac{1}{\alpha}}$  is the  $\alpha$ -norm of the density  $f$ . In (6), equality holds if

$$\lambda(q) = f^{\frac{d}{d+r}}(q) / \int_{\mathbb{R}^d} f^{\frac{d}{d+r}}(q') dq', \quad \forall q \quad (7)$$

Therefore, the minimum distortion  $\kappa_{rd}n^{-\frac{r}{d}}\|f\|_{\frac{d}{d+r}} + o(n^{-\frac{r}{d}})$  is achieved by the point density function in (7).

### B. The UAV Case $h > 0$

We now consider the case  $h > 0$ . We begin with the simple case of a uniform one-dimensional distribution. The proof of the following proposition can be found in Appendix A.

**Proposition 2.** *Let  $f(q) = \mathbf{1}(q \in [0, 1])$ . A minimizer of (1) is the uniform quantizer codebook  $\mathbf{x}_u$ . The corresponding minimum average power is*

$$P(\mathbf{x}_u, f) = 2n \int_0^{\frac{1}{2n}} (u^2 + h^2)^{\frac{r}{2}} du. \quad (8)$$

For a general  $d$  and  $f$ , we observe that if  $x_1, \dots, x_n$  is an optimal deployment, the set of points  $q$  with the property that  $\min_i \|q - x_i\| \rightarrow 0$  as  $n \rightarrow \infty$  has probability one.<sup>1</sup> This amounts to the intuitive observation that every GT should be allocated a closer UAV as the number of available UAVs grows to infinity. As a result, we may use the Taylor series expansion

$$\left( \min_i \|x_i - q\|^2 + h^2 \right)^{\frac{r}{2}} = h^r + \frac{1}{2} r h^{r-2} \min_i \|x_i - q\|^2 + o\left( \min_i \|x_i - q\|^2 \right) \quad (9)$$

so that, substituting to (1), we have

$$P(\mathbf{x}, f) = h^r + \frac{1}{2} r h^{r-2} \int_{\mathbb{R}^d} \min_i \|x_i - q\|^2 f(q) dq + \int_{\mathbb{R}^d} o\left( \min_i \|x_i - q\|^2 \right) f(q) dq. \quad (10)$$

Using (6) and (7), we can then obtain the following theorem.

**Theorem 1.** *As  $n \rightarrow \infty$ , we have*

$$P^*(f) = \begin{cases} \kappa_{rd}n^{-\frac{r}{d}}\|f\|_{\frac{d}{d+r}} + o(n^{-\frac{r}{d}}), & h = 0, \\ h^r + \frac{r h^{r-2} \kappa_{2d}}{2} n^{-\frac{2}{d}}\|f\|_{\frac{d}{d+2}} + o(n^{-\frac{2}{d}}), & h > 0. \end{cases} \quad (11)$$

*The optimal point density function is given by*

$$\lambda^*(q; f) \triangleq \begin{cases} f^{\frac{d}{d+r}}(q) / \int_{\mathbb{R}^d} f^{\frac{d}{d+r}}(q') dq', & h = 0, \\ f^{\frac{d}{d+2}}(q) / \int_{\mathbb{R}^d} f^{\frac{d}{d+2}}(q') dq', & h > 0. \end{cases} \quad (12)$$

<sup>1</sup>Otherwise, there is a constant  $a > 0$  such that with some positive probability  $\epsilon > 0$ , one has  $\min_i \|q - x_i\| > a$  infinitely often. This implies  $P^*(f) > \epsilon a$  infinitely often, contradicting Proposition 1.

This provides a complete asymptotic characterization of the achievable GT power consumption and the corresponding optimal UAV configuration.

#### IV. OPTIMIZATION OF A DYNAMIC DEPLOYMENT: EXTREMAL CASES

We now consider the dynamic scenario, where the GT density varies periodically over time. As discussed in Section II-B, the goal in this case is to minimize the time-averaged power consumption  $Q$  in (2), subject to the constraint  $\sum_{i=1}^n M_i \leq M$  on the total movement of UAVs. Here,  $M_i$  denotes the total movement of the  $i$ th UAV, and has been defined in (3). Given  $M \geq 0$ , we use the notation  $Q^*(M)$  to denote the minimum of (2) subject to  $\sum_{i=1}^n M_i \leq M$ . In this section in particular, we consider the two extremal cases  $M = 0$  and  $M \rightarrow \infty$ . The remaining moderate cases will be discussed in Section V.

##### A. No UAV movement: $M = 0$

The case  $M = 0$  corresponds to a scenario where we do not allow any UAV movement. Equivalently, the UAV locations are fixed over time as  $\mathbf{x}_t = \mathbf{x}'$ ,  $\forall t$  for a collection  $\mathbf{x}' = [x'_1 \cdots x'_n]$  of UAV locations to be optimized. By (1) and (2), we have

$$Q^*(0) = \min_{\mathbf{x}'} \frac{1}{T} \int_0^T \int_{\mathbb{R}^d} \min_i (\|x'_i - q\|^2 + h^2)^{\frac{r}{2}} f_t(q) dq dt. \quad (13)$$

Now, let  $\bar{f}(q) \triangleq \frac{1}{T} \int_0^T f_t(q) dt$  be the ‘‘time-averaged density.’’ Note that  $\int_{\mathbb{R}^d} \bar{f}(q) dq = 1$  so that  $\bar{f}$  is a valid density function. According to (1) and (13), we have  $Q^*(0) = \min_{\mathbf{x}'} P(\mathbf{x}', \bar{f})$ , and optimizing over  $\mathbf{x}'$  leads to the following.

**Proposition 3.** *We have  $Q^*(0) = P^*(\bar{f})$ .*

Note that Theorem 1 can be applied to provide an asymptotically tight expression for  $P^*(\bar{f})$  (and thus  $Q^*(0)$ ).

**Example 1.** *Let us consider a one-dimensional network  $d = 1$ , a period of length  $T = 2$  with path loss exponent  $r = 2$ . For a simpler exposition, we further consider an UGV network where  $h = 0$ . Let the time-varying GT density be given by*

$$f_t(q) = (1 + 3|t|)(q - 2 + 2|t|)^{3|t|}, \quad q \in [2 - 2|t|, 3 - 2|t|], \quad t \in [-1, 1]. \quad (14)$$

This defines shifted power-law densities. For example for  $t = -1$ , we obtain the density  $f_1(q) = 4q^3$ ,  $q \in [0, 1]$ , and for  $t = 0$ , we obtain  $f_0(q) = 1$ ,  $q \in [2, 3]$ . The time-averaged density  $\bar{f}$  as well as its  $\frac{1}{3}$ -norm  $\|\bar{f}\|_{\frac{1}{3}} \approx 6.08$  can be found by numerical integration. By Proposition 3 and Theorem 1, it follows that  $Q^*(0) \approx \frac{6.08}{12}n^{-2} = 0.507n^{-2}$ . The optimal point (UAV) density function is given by  $\lambda^*(q, \bar{f})$ , as defined in (12).  $\square$

### B. Unlimited UAV movement: $M \rightarrow \infty$

We now allow an unlimited amount of UAV movement so as to obtain the minimum possible time-averaged GT power consumption. For this purpose, at each time  $t$ , we use the UAV locations that provide the minimum “instantaneous” GT power consumption. This results in the time-averaged power

$$Q^*(\infty) = \frac{1}{T} \int_0^T P^*(f_t) dt. \quad (15)$$

We recall that Theorem 1 provides an asymptotic expression for the integrand  $P^*(f_t)$ . This can be substituted to (15) for an asymptotically tight characterization of  $Q^*(\infty)$ .

We now argue that (15) is, in fact, achievable with a finite amount of total movement as well. In other words, there is a constant  $\bar{M} > 0$  such that  $Q^*(M) = Q^*(\infty)$  for every  $M \geq \bar{M}$ . The idea is to observe that the GT density  $f_t$  at time  $t$  is not “vastly different” than the GT density  $f_{t+dt}$  at time  $t + dt$ . This stems from our practical assumption in Section II-B that the spatiotemporal density  $f_t(q)$  is continuous in both space and time. As a result, we expect the optimal location for each UAV to be a well-behaved continuous function of time, resulting in a finite amount of total UAV movement.

We utilize high-resolution quantization theory to estimate  $\bar{M}$ . The key is to recover the location of each UAV at any given point  $t$  in time through the optimal quantizer point density function at time  $t$ . Namely, let  $\mathbf{x}_t^* \triangleq [x_{t,1}^* \cdots x_{t,n}^*]$  denote the optimal UAV locations at time  $t$  for density  $f_t$ . We first consider the case of one dimension  $d = 1$ . Without loss of generality, suppose  $x_{t,1}^* \leq \cdots \leq x_{t,n}^*$ . Given  $x \in [0, 1]$ , let  $\Lambda_{\text{inv}}^*(x; f_t)$  be the unique real number that satisfies

$$\int_0^{\Lambda_{\text{inv}}^*(x; f_t)} \lambda^*(q; f_t) dq = x, \quad (16)$$

where  $\lambda^*(q; f_t)$  is the optimal point density function for  $f_t$ , as defined in (12) of Theorem 1. Note that  $\Lambda_{\text{inv}}^*(x; f_t)$  is the inverse of the cumulative distribution function  $u \rightarrow \int_0^u \lambda^*(q; f_t) dq$ . Our idea is to approximate the optimal UAV locations via

$$x_{t,i}^* \simeq \tilde{x}_{t,i} \triangleq \Lambda_{\text{inv}}^* \left( \frac{2i-1}{2n}; f_t \right), \quad i = 1, \dots, n. \quad (17)$$

Note that if  $U$  is a random variable that is uniformly distributed on  $[0, 1]$ , then, according to the inverse transform sampling method, the random variable  $\Lambda_{\text{inv}}^*(U; f_t)$  is distributed according to the density function  $\lambda^*(q, f_t)$ . The transformation in (17) can thus be considered to be a ‘‘deterministic version’’ of inverse transform sampling, where the uniform random variable  $U$  is replaced with the uniform quantizer with reproduction points  $\frac{2i-1}{2n}$ ,  $i = 1, \dots, n$ . The resulting estimates  $\tilde{x}_{t,1}, \dots, \tilde{x}_{t,n}$  are consistent with the density function  $\lambda^*(q; f_t)$  in the sense that for every  $q$  and  $\epsilon > 0$ , the fraction  $\frac{1}{n} |\{i : \tilde{x}_{t,i} \in (q, q + \epsilon)\}|$  of UAVs that are located on  $(q, q + \epsilon)$  converges to  $\lambda^*(q; f_t)\epsilon$  as  $n \rightarrow \infty$ .

Substituting (17) to (3), we obtain the following result.

**Theorem 2.** *Let  $d = 1$ . As  $n \rightarrow \infty$ , the minimum possible average power consumption of  $Q^*(\infty) = \frac{1}{T} \int_0^T P^*(f_t)$  is achievable with a total movement of*

$$\overline{M}_i \triangleq \frac{1}{T} \int_0^T \left| \frac{\partial \Lambda_{\text{inv}}^* \left( \frac{2i-1}{2n}; f_t \right)}{\partial t} \right| dt \quad (18)$$

for the  $i$ th UAV. Correspondingly,  $\overline{M} = \sum_{i=1}^n \overline{M}_i$ .

**Example 2.** *We continue the setup in Example 1. We have*

$$\|f_t\|_{\frac{1}{3}} = (1 + 3|t|) \left( \int_{2-2|t|}^{3-2|t|} (q - 2 + 2|t|)^{|t|} dq \right)^3 = (1 + 3|t|) \left( \int_0^1 q^{|t|} dq \right)^3 = \frac{1 + 3|t|}{(1 + |t|)^3}. \quad (19)$$

This yields

$$Q^*(\infty) = \frac{1}{2} \int_{-1}^1 P^*(f_t) dt = \frac{1}{24n^2} \int_{-1}^1 \|f_t\|_{\frac{1}{3}} dt + o\left(\frac{1}{n^2}\right) \quad (20)$$

$$= \frac{1}{24n^2} \int_{-1}^1 \frac{1 + 3|t|}{(1 + |t|)^3} dt + o\left(\frac{1}{n^2}\right) = \frac{1}{16n^2} + o\left(\frac{1}{n^2}\right). \quad (21)$$

The first three equalities follow from (15), (11), and (19), respectively. In order to estimate  $\overline{M}$ , we use the formula (12) to first calculate  $\lambda^*(q, f_t) = (1 + |t|)(q - 2 + 2|t|)^{|t|}$ . In the light of (16), we then solve for  $\theta$  in the integral equality

$$\int_0^\theta (1 + |t|)(q - 2 + 2|t|)^{|t|} dq = x \quad (22)$$

to obtain the inverse cumulative distribution function

$$\Lambda_{\text{inv}}^*(x, f_t) = \theta = 2 - 2|t| + x^{\frac{1}{1+|t|}}, \quad x \in [0, 1], \quad t \in [-1, 1]. \quad (23)$$

According to (17), we can then obtain

$$\tilde{x}_{t,i} = \Lambda_{\text{inv}}^* \left( \frac{2i-1}{2n}; f_t \right) = 2 - 2|t| + \left( \frac{2i-1}{2n} \right)^{\frac{1}{1+|t|}}, \quad i = 1, \dots, n. \quad (24)$$

Note that, for a fixed index  $i$ , the function  $t \mapsto \tilde{x}_{t,i}$  is symmetric around the origin and decreases on  $[0, 1]$ . Theorem 2 combined with the fundamental theorem of calculus then yields

$$\overline{M}_i = \frac{1}{2} \int_{-1}^1 \left| \frac{\partial \tilde{x}_{t,i}}{\partial t} \right| dt = \tilde{x}_{0,i} - \tilde{x}_{1,i} = 2 + \frac{2i-1}{2n} - \left( \frac{2i-1}{2n} \right)^{\frac{1}{2}}. \quad (25)$$

Thus, the power consumption of  $Q^*(\infty)$  is achievable with a total UAV movement of

$$\overline{M} = \sum_{i=1}^n \overline{M}_i = 2n + \sum_{i=1}^n \left( \frac{2i-1}{2n} - \left( \frac{2i-1}{2n} \right)^{\frac{1}{2}} \right), \quad (26)$$

and the optimal UAV trajectories are given by  $\tilde{x}_{t,i}$  in (24). Note that, as  $n \rightarrow \infty$ , we have

$$\frac{\overline{M}}{n} \rightarrow 2 + \int_0^1 (x - \sqrt{x}) dx = \frac{11}{6}. \quad (27)$$

Therefore, for a per-UAV movement of  $\frac{11}{6}$ , a GT power consumption of roughly  $\frac{1}{16n^2}$  is achievable.

On the other hand, Example 1 shows that without any UAV movement, a GT power consumption of roughly  $\frac{0.507}{n^2}$  is achievable. For the particular scenario in Examples 1 and 2, allowing mobility of access points thus potentially yields an 8-fold reduction in the GT power consumption.  $\square$

The arguments that we have used to obtain Theorem 2 are not immediately applicable to the case of two dimensions. The main difficulty is to find a simple analogue of (17) that can faithfully extract the optimal UAV locations from the optimal UAV density functions. We leave a resolution of this problem as future work. Nevertheless,  $\overline{M}$  and  $Q^*(\overline{M})$  can still be numerically approximated for two dimensional densities as we show in Section VI.

## V. OPTIMIZATION OF A DYNAMIC DEPLOYMENT: MODERATE DISTANCES

We recall that our goal in the dynamic deployment scenario is to find the minimum average GT power consumption  $Q^*(M)$  subject to the total movement constraint  $M$  on the UAVs. In the previous section, we have analytically characterized the achievable performance in the extremal cases of no UAV movement  $M = 0$  and unlimited UAV movement  $M = \infty$ . In particular, we have shown that there exists a sufficient amount of total movement  $\bar{M}$  such that  $Q^*(\bar{M}) = Q^*(\infty)$ . We now consider the achievable performance between the two extremal cases. In other words, we consider the moderate distances regime  $0 < M < \bar{M}$ .

A precise analytical characterization of the achievable performance appears to be very challenging for the case  $0 < M < \bar{M}$ . We thus mainly follow a numerical approach. Specifically, we introduce a Lagrangian-based descent algorithm for trajectory optimization. We first present the general strategy and outline of the algorithm.

### A. Outline of an Algorithm for Trajectory Optimization

Our general strategy for trajectory optimization is to follow the classical Lagrangian approach of constrained optimization. Namely, we combine the power consumption (objective) function  $Q$  in (2) and the movement (constraint) function  $\sum_{i=1}^n M_i$  through the Lagrangian

$$Q + \ell \sum_{i=1}^n M_i = \frac{1}{T} \int_0^T \left[ P(\mathbf{x}_t, f_t) + \ell \sum_{i=1}^n \sqrt{\sum_{j=1}^d \left| \frac{\partial x_{t,i,j}}{\partial t} \right|^2} \right] dt. \quad (28)$$

Minimizing the Lagrangian for different values of the Lagrange multiplier  $\ell > 0$  enables travel over the  $(M, Q^*(M))$  tradeoff curve: For example, a small  $\ell$  does not penalize the total amount of movement as much as a larger  $\ell$  does. It thus results in a lower power consumption compared to the case of a larger  $\ell$ , albeit at the expense of more movement. The formulation in (28) thus resembles the Lagrangian formulation of the entropy-constrained quantizer design problem [39].

Minimizing (28) requires optimization over the uncountably infinitely many variables  $x_{t,i}$ ,  $t \in [0, T]$ ,  $i \in \{1, \dots, n\}$ , and is thus infeasible. The first step towards a feasible optimization is

to discretize the continuous time interval  $[0, T]$  to the set of discrete time instances  $\{\frac{kT}{K} : k \in \{0, \dots, K-1\}\}$ , where  $K \geq 2$  is a natural number. This results in the discrete-time Lagrangian

$$\mathcal{L} \triangleq \frac{1}{K} \sum_{k=0}^{K-1} P(\mathbf{y}_k, \hat{f}_k) + \frac{\ell}{K} \sum_{k=0}^{K-1} \sum_{i=1}^n \|y_{k,i} - y_{k-1,i}\|, \quad (29)$$

where the discrete time  $k$  corresponds to the continuous time  $\frac{kT}{K}$ , and the optimization is over  $\mathbf{y}_k \triangleq \mathbf{x}_{\frac{kT}{K}} = [y_{k,1} \cdots y_{k,n}]$  with density  $\hat{f}_k \triangleq f_{\frac{kT}{K}}$ . Also, for a simple notation, we have omitted to indicate that all  $k$ -dependent indices are evaluated modulo  $K$ . For example, for  $k = 0$ , the discrete time index  $k - 1 = -1$  is the same as the discrete time index  $-1 \bmod K = K - 1$ .

It can be shown that, under some technical conditions on  $x_{t,i}$ ,  $i = 1, \dots, n$  and  $f_t$ , such as continuity in  $t$ , the discrete time Lagrangian converges to the continuous time Lagrangian as the number of time steps  $K$  grows to infinity. We thus expect the minimizers of (29) and (28) to coincide asymptotically as  $K \rightarrow \infty$ . Still, the direct minimization of (29) is a  $dnK$  dimensional optimization problem. In order to further reduce the dimensionality, we define

$$\mathcal{L}_k \triangleq \frac{1}{K} P(\mathbf{y}_k, \hat{f}_k) + \frac{\ell}{K} \sum_{i=1}^n \|y_{k,i} - y_{k-1,i}\| + \frac{\ell}{K} \sum_{i=1}^n \|y_{k,i} - y_{k+1,i}\|, k = 1, \dots, K, \quad (30)$$

and note that  $\mathcal{L}$  depends on  $\mathbf{y}_k$  only through  $\mathcal{L}_k$ . The quantity  $\mathcal{L}_k$  can be considered to be the Lagrangian cost at time instance  $k$ . Our algorithm is then to perform alternating optimization over the discrete time instances. In detail, we begin with an initial (for example, random) guess on the trajectories  $\mathbf{y}_0, \dots, \mathbf{y}_{K-1}$ . For the infinite sequence of time indices  $k = 0, 1, \dots, K-1, 0, 1, \dots, K-1, \dots$ , we minimize  $\mathcal{L}_k$  over  $\mathbf{y}_k$ , while keeping all  $\mathbf{y}_i$ ,  $i \neq k$  fixed (The specific manner in which we perform the minimization will be discussed later on). Since each step minimizes  $\mathcal{L}_k$  over  $\mathbf{y}_k$  for some  $k \in \{0, \dots, K-1\}$ , and the dependence of  $\mathcal{L}$  on  $\mathbf{y}_k$  is only through  $\mathcal{L}_k$ , the process guarantees a non-increasing  $\mathcal{L}$ . It follows that the algorithm converges in a cost function sense. In fact, in our numerical experiments, we have observed that the algorithm also provides convergent trajectories as well. A formal proof of this observation will remain as an interesting direction for future research.

The pseudocode of our trajectory optimization algorithm is as shown in Algorithm 1. We call one pass over all discrete time instances as one epoch of optimization. The algorithm terminates

---

**Algorithm 1** Trajectory Optimization
 

---

- 1: Initialize  $\mathbf{y}_0, \dots, \mathbf{y}_{K-1}$ . Set maxEpochs.
  - 2: **for** epochs = 1 **to** maxEpochs **do**
  - 3:   Update the UAV deployments as  $\mathbf{y}_k \leftarrow \arg \min_{\mathbf{y}_k} \mathcal{L}_k$ ,  $k = 0, \dots, K - 1$ .
  - 4: **end for**
- 

after a certain number of epochs that is to be chosen depending on the input parameters. Different termination criteria (such as the convergence of trajectories or the cost  $\mathcal{L}$ ) can also be considered. Obviously, due to the non-convex non-linear nature of the trajectory optimization problem, the resulting trajectory may not necessarily be the globally-optimal solution.

### B. Minimizing the Lagrangian Cost at a Given Time Instance

We now seek a computationally-efficient solution for the  $dn$ -dimensional optimization problem of minimizing the Lagrangian cost  $\mathcal{L}_k$  in (30). In other words, we study the optimization problems in Line 3 of Algorithm 1. We follow the same decomposition strategy as in Section V-A. This will lead us to a variant of the Lloyd algorithm of vector quantization [32], [33]. First, for the term  $P(\mathbf{y}_k, \hat{f}_k)$  in (30), we recall from (1) that

$$P(\mathbf{y}_k, \hat{f}_k) = \int_{\mathbb{R}^d} \min_i (\|y_{k,i} - q\|^2 + h^2)^{\frac{\tau}{2}} \hat{f}_k(q) dq \quad (31)$$

$$= \sum_{i=1}^n \int_{\mathcal{V}_{k,i}} (\|y_{k,i} - q\|^2 + h^2)^{\frac{\tau}{2}} \hat{f}_k(q) dq, \quad (32)$$

where  $\mathcal{V}_{k,i} \triangleq \{q : \|y_{k,i} - q\| \leq \|y_{k,j} - q\|, \forall j \in \{1, \dots, n\}\}$  is the Voronoi cell of the  $i$ th UAV at time  $k$ . Given that the Voronoi cells  $\mathcal{V}_{k,i}$ ,  $i = 1, \dots, n$  are kept fixed, it follows that for any given UAV index  $i \in \{1, \dots, n\}$ , the expression (30) depends on  $y_{k,i}$  only through the quantity

$$\mathcal{L}_{k,i} \triangleq \frac{1}{K} \int_{\mathcal{V}_{k,i}} (\|y_{k,i} - q\|^2 + h^2)^{\frac{\tau}{2}} \hat{f}_k(q) dq + \frac{\ell}{K} \|y_{k,i} - y_{k-1,i}\| + \frac{\ell}{K} \|y_{k,i} - y_{k+1,i}\|. \quad (33)$$

The quantity  $\mathcal{L}_{k,i}$  can be interpreted as the Lagrangian cost of UAV  $i$  at discrete time instance  $k$ . In general, given that  $\mathcal{V}_{k,i}$ ,  $i = 1, \dots, n$  are kept fixed,  $\mathcal{L}_{k,i}$  is a convex function of  $y_{k,i}$  and

thus be effectively minimized using any convex optimization method, or gradient descent. For reference, the gradient of  $\mathcal{L}_{k,i}$  with respect to  $y_{k,i}$  can be calculated to be

$$\frac{\partial \mathcal{L}_{k,i}}{\partial y_{k,i}} = \frac{r}{K} \int_{\mathcal{V}_{k,i}} (\|y_{k,i} - q\|^2 + h^2)^{\frac{r}{2}-1} (y_{k,i} - q) \hat{f}_k(q) dq + \frac{\ell}{K} \frac{y_{k,i} - y_{k-1,i}}{\|y_{k,i} - y_{k-1,i}\|} + \frac{\ell}{K} \frac{y_{k,i} - y_{k+1,i}}{\|y_{k,i} - y_{k+1,i}\|}. \quad (34)$$

As we shall soon discuss, further simplifications or even closed-form solutions to the problem of minimizing  $\mathcal{L}_{k,i}$  are available in certain special cases. Regardless, once each  $\mathcal{L}_{k,i}$ ,  $i = 1, \dots, n$  are minimized (while keeping  $\mathcal{V}_{k,i}$ ,  $i = 1, \dots, n$  fixed), the new Voronoi regions  $\mathcal{V}_{k,i}$ ,  $i = 1, \dots, n$  will be calculated according to the new  $y_{k,i}$ ,  $i = 1, \dots, n$ . Algorithm 2 summarizes this process of minimizing  $\mathcal{L}_k$ . The algorithm proceeds in an iterative manner until a certain maximum number of iterations is reached. Since each optimization we have described results in a non-increasing  $\mathcal{L}_k$ , Algorithm 2 converges in a cost function sense.

---

**Algorithm 2** Minimizing  $\mathcal{L}_k$

---

- 1: Initialize UAV locations  $\mathbf{y}_k = [y_{k,1} \cdots y_{k,n}]$ . Set `maxIterations`.
  - 2: **for** `iterations = 1` **to** `maxIterations` **do**
  - 3:   Calculate the Voronoi regions  $\mathcal{V}_{k,i}$ ,  $i = 1, \dots, n$ .
  - 4:   Update the UAV locations as  $y_{k,i} \leftarrow \arg \min_{y_{k,i}} \mathcal{L}_{k,i}$ ,  $i = 1, \dots, n$ .
  - 5: **end for**
- 

### C. Minimizing the Lagrangian Cost of a UAV at a Given Time Instance

We now consider the minimization of  $\mathcal{L}_{k,i}$  for a given UAV index  $k$  and time instance  $i$ . This problem appears in Line 4 of Algorithm 2. As we have mentioned in Section V-B, in general,  $\mathcal{L}_{k,i}$  in (33) can be minimized using gradient descent. Here, we point out that the minimization becomes considerably simpler for the special case  $r = 2$  of the path loss exponent. In fact, we will also provide a closed-form solution for  $r = 2$  and one-dimensional networks  $d = 1$ .

Let us first note that for any set  $A$  and vector  $x$ , we have

$$\int_A \|x - q\|^2 f(q) dq = \int_A (\|x\|^2 - 2x^T q + \|q\|^2) f(q) dq \quad (35)$$

$$= \|x\|^2 \left( \int_A f(q) dq \right) - 2x^T \left( \int_A qf(q) dq \right) + \int_A \|q\|^2 f(q) dq \quad (36)$$

$$= \left( \int_A f(q) dq \right) \left\| x - \frac{\int_A qf(q) dq}{\int_A f(q) dq} \right\|^2 + \int_A \|q\|^2 f(q) dq - \frac{\left\| \int_A qf(q) dq \right\|^2}{\int_A f(q) dq}. \quad (37)$$

Note that the last two terms do not depend on  $x$ . When  $r = 2$ , we use the identity in (37) to rewrite the integral in (33). Then, by removing the terms that do not depend on  $y_{k,i}$ , it follows that the minimization of (33) over  $y_{k,i}$  is equivalent to minimizing

$$\phi(x) \triangleq \|x - u\| + \|x - v\| + c\|x - w\|^2 \quad (38)$$

over all  $x$ , where the constant vectors  $u, v, w$ , and the scalar  $c$  are given by

$$u \triangleq y_{k-1,i}, \quad v \triangleq y_{k+1,i}, \quad w \triangleq \frac{\int_{\mathcal{V}_{k,i}} q \hat{f}_k(q) dq}{\int_{\mathcal{V}_{k,i}} \hat{f}_k(q) dq}, \quad c \triangleq \frac{1}{\ell} \int_{\mathcal{V}_{k,i}} \hat{f}_k(q) dq. \quad (39)$$

Therefore, when we wish to minimize (33) (by using gradient descent for example), we can avoid integration over the generally complicated region  $\mathcal{V}_{k,i}$  by instead considering the equivalent problem of minimizing (38). Let us further note that the domain/search space of minimization of (38) is the entire  $\mathbb{R}^d$ . We can also greatly reduce the size of this search space. For this purpose, we need the following lemma, whose proof can be found in Appendix B.

**Lemma 1.** *Let  $T \subset \mathbb{R}^d$  be a triangle with vertices  $u, v, w$ , including its boundary and interior. For any  $x \in \mathbb{R}^d$ , there exists  $y \in T$  such that  $\|y - a\| \leq \|x - a\|$  for every vertex  $a$  of  $T$ .*

We now have the following proposition.

**Proposition 4.** *A minimizer  $x^*$  of (38) lies on the triangle  $T$  with vertices  $u, v, w$ .*

*Proof.* Suppose  $x^* \notin T$ . By Lemma 1, we can find  $y \in T$  such that  $\|y - a\| \leq \|x^* - a\|$  for every vertex  $a$  of  $T$ . It follows that  $y$  is also a minimizer of (38).  $\square$

Therefore, without loss of optimality, we may minimize (38) over all  $x$  of the form  $x = w + \alpha x' + \beta x''$ , where  $\alpha, \beta \geq 0$ ,  $\alpha + \beta \leq 1$ , and  $x' = u - w$ ,  $x'' = v - w$  are triangle edge vectors. Hence, the minimization of (38), which should take place over the entire  $\mathbb{R}^d$ , can be transformed to a convex optimization over the (two-dimensional) triangle  $\alpha, \beta \geq 0$ ,  $\alpha + \beta \leq 1$ .

In the special case of one dimension, a minimizer of (38) can be found in closed form. This is shown by the following proposition, whose proof can be found in Appendix C.

**Proposition 5.** *Let  $d = 1$ , and  $x^* = \arg \min_{x \in \mathbb{R}^d} \phi(x)$ . For a simpler notation, we define the intermediate variables*

$$u' \triangleq \min\{u, v\}, \quad v' \triangleq \max\{u, v\}, \quad \alpha \triangleq \min \left\{ \left| w - \frac{u+v}{2} \right|, \frac{1}{c} \right\}. \quad (40)$$

We have

$$x^* = \begin{cases} w, & w \in [u', v'], \\ \max\{v', w - \alpha\}, & w > v', \\ \min\{u', w + \alpha\}, & w < u'. \end{cases} \quad (41)$$

As a result, for  $d = 1$  and  $r = 2$ , the entire trajectory optimization algorithm can be implemented with very low computational complexity.

## VI. NUMERICAL RESULTS

In this section, we provide numerical simulations that verify our analytical results. We first consider the scenario in Examples 1 and 2. For reader's convenience, we recall that given  $n$  UAVs and no UAV movement, our analysis suggests that the best possible GT power consumption in this scenario is given by

$$Q^*(0) \approx \frac{6.08}{12} \frac{1}{n^2} + o\left(\frac{1}{n^2}\right) = \frac{0.507}{n^2} + o\left(\frac{1}{n^2}\right). \quad (42)$$

On the other hand, with an unlimited UAV movement, the best GT power consumption is

$$Q^*(\infty) = \frac{1}{16n^2} + o\left(\frac{1}{n^2}\right). \quad (43)$$

In fact, the performance in (43) is achievable with a per-UAV movement of

$$\frac{\bar{M}}{n} = 2 + \frac{1}{n} \sum_{i=1}^n \left( \frac{2i-1}{2n} - \left( \frac{2i-1}{2n} \right)^{\frac{1}{2}} \right) \rightarrow \frac{11}{6} \text{ as } n \rightarrow \infty. \quad (44)$$

For the same scenario, in Fig. 2, we show the simulated tradeoff between the per-UAV movement and GT power consumption for different number of UAVs. The horizontal axis represents the distance traveled per UAV, and the vertical axis represents the GT power consumption in

logarithmic scale. Each marked data point is obtained using the algorithm in Section V with a time discretization of  $K = 20$  and different values of the Lagrange multiplier  $\ell$ . The continuous-time trajectory is reconstructed from the discrete-time trajectory using linear interpolation.

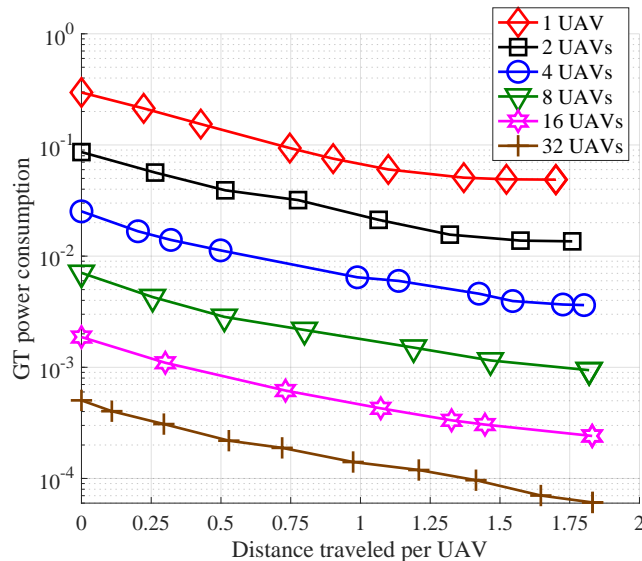


Fig. 2: GT power consumptions for different per-UAV movements in a one-dimensional network.

We can observe that, doubling the number of UAVs roughly quarters the average GT power consumption for the same amount of distance traveled per UAV. The  $O(\frac{1}{n^2})$  decay of the analytical formulae in (42) and (43) justify this observation for the two special cases of zero and unlimited UAV movement, respectively. The same decay rate can be observed if one instead considers a total movement constraint instead of a per-UAV movement constraint.

In Fig. 3, we show the average GT power consumption for different number of UAVs and the extremal scenarios of zero and unlimited UAV movements. The logarithmically-scaled horizontal and the vertical axes represent the number of UAVs and the GT power consumptions, respectively. Note that, the simulation curves for zero and unlimited UAV movements respectively correspond to the vertical coordinates of the leftmost and the rightmost data points in Fig. 2. We can observe that the analytical results in (42) and (43) match almost perfectly with the simulations. Due to its asymptotic nature, the analysis is more accurate when the number of UAVs is large.

In Fig. 4, we show the per-UAV traveled distances for the scenario of unlimited UAV move-

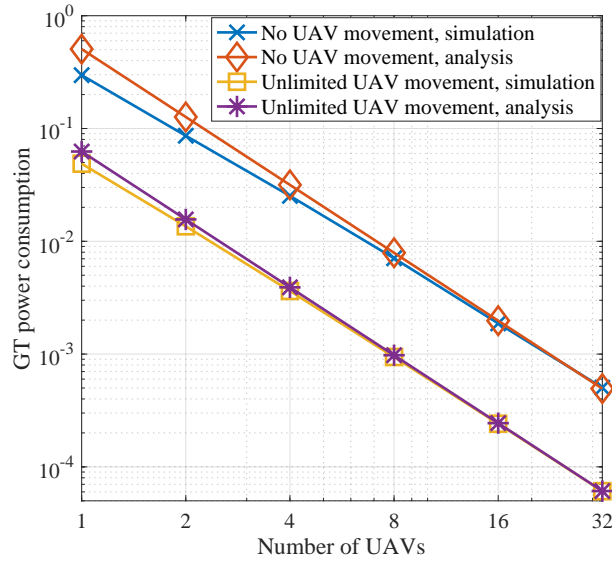


Fig. 3: GT power consumptions in extremal cases for a one-dimensional network.

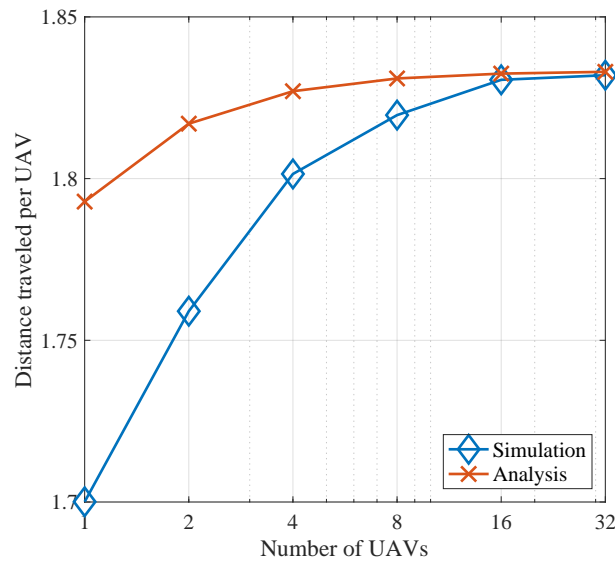


Fig. 4: Distance per UAV for different number of UAVs with unlimited movement.

ment. The simulation curve corresponds to the horizontal coordinates of rightmost data points in Fig. 2, and the analysis curve corresponds to the formula (44). Noting that the values in the vertical axis of the figure are already very close, we can conclude that the analysis matches simulation very well. Example 2 also provides the optimal trajectories for the unlimited movement scenario in (24). In Fig. 5, we compare these analytical trajectories with the trajectories

that are obtained numerically for the special case of 8 UAVs. The horizontal and the vertical axes represent the time, and the UAV locations respectively. Each curve represents the trajectory of one UAV. We have normalized both the analytical and the simulation trajectories by subtracting the time-varying drift  $2 - 2|t|$  of the density function. We can observe that, for any UAV index, the analysis matches the simulation very well.

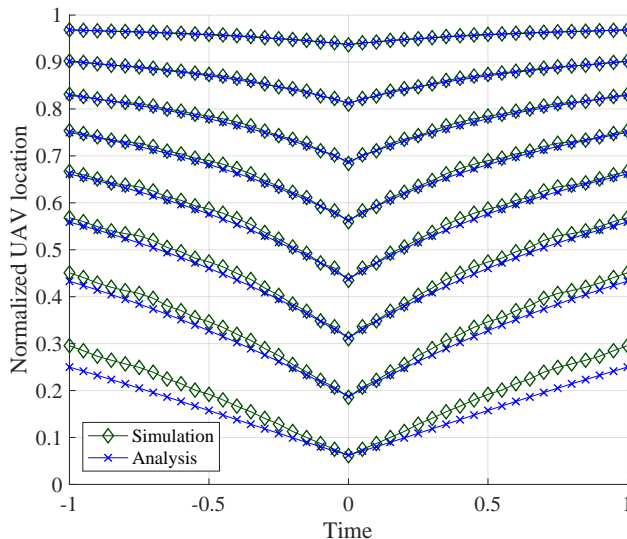


Fig. 5: Trajectories of 8 UAVs in a one-dimensional network.

As an example of two-dimensional ( $d = 2$ ) dynamic deployment, let  $f_t$  be the density function of the random variable  $(3 + 2 \sin 2\pi t)N + 10[\sin 2\pi t \ \cos 2\pi t]$ , where  $N$  is a Gaussian random vector with identity covariance matrix. Hence,  $f_t$  is Gaussian at any  $t$  and its mean and variance varies periodically over time with  $T = 1$ . We consider a path loss exponent of  $r = 3$ , and UAV height  $h = 10$ . The normalized second moment of the origin-centered hexagon can be calculated to be  $\kappa_{22} = \frac{5}{18\sqrt{3}}$ . By Theorems 1 and 2, the asymptotic GT power consumptions are then

$$Q^*(0) = 1000 + \frac{25}{6\sqrt{3}} \frac{\|\bar{f}\|_{\frac{1}{2}}}{n} + o\left(\frac{1}{n}\right), \quad (45)$$

and

$$Q^*(\infty) = 1000 + \frac{25}{6\sqrt{3}} \frac{\int_0^1 \|f_t\|_{\frac{1}{2}} dt}{n} + o\left(\frac{1}{n}\right), \quad (46)$$

for the cases of zero and unlimited UAV movement, respectively. In (45), the half-norm  $\|\bar{f}\|_{\frac{1}{2}}$  can be calculated through numerical integration to be roughly 908.16. For the case of unlimited movement in (46), after some calculus, we can obtain  $\int_0^1 \|f_t\|_{\frac{1}{2}} dt = 88\pi$  in closed form.

As the asymptotic expressions (45) and (46) also show, the choice of parameters  $r = 3$  and  $h = 10$  imply that the GT power consumption is at least  $h^r = 1000$  regardless of the constraints on the total UAV movement. For a clear illustration of results, we thus normalize the GT transmission power by subtracting 1000 from the true GT transmission power.

In Fig. 6, we show the tradeoff between the per-UAV movement and the normalized GT power consumption for different number of UAVs. Unlike the case of the one-dimensional network shown earlier, for a fixed per-UAV movement, doubling the number of UAVs roughly only halves (instead of quartering) the normalized GT power consumption. The asymptotic expression in (45) formally verifies this observation for the special case of zero movement.

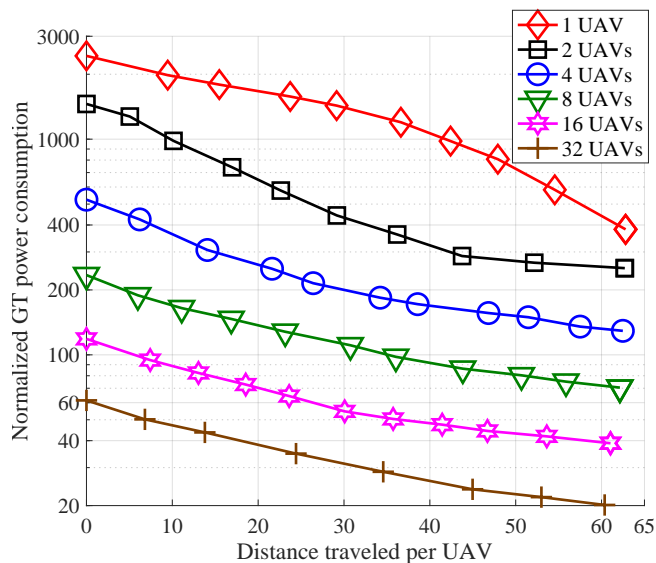


Fig. 6: GT power consumptions for different per-UAV movements in a two-dimensional network.

In Fig. 7, we show the average GT power consumption for different number of UAVs in the zero and unlimited UAV movement scenarios. We can observe that the analytical results in (45) and (46) match very well with the simulations. Even though the analysis will provide an asymptotically tight approximation on the simulation results, the amount of mismatch for a

moderate number of UAVs is more pronounced compared to the case of the one-dimensional network. The reason is the lesser amount of UAVs per dimension. One encounters the same phenomenon in the performance analysis of general vector quantizers.

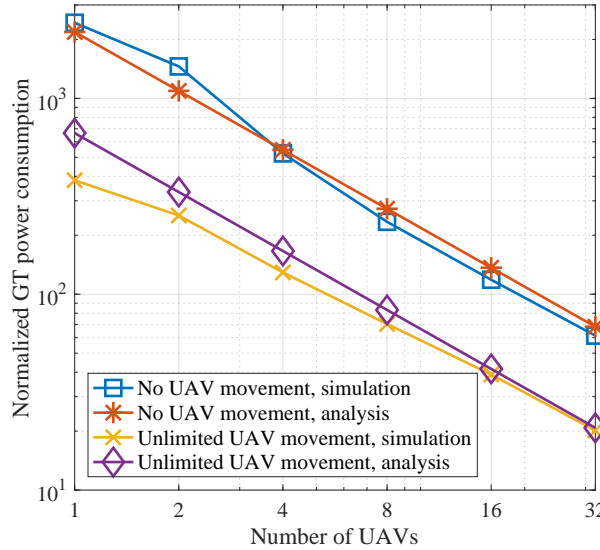


Fig. 7: GT power consumptions in extremal cases for a two-dimensional network.

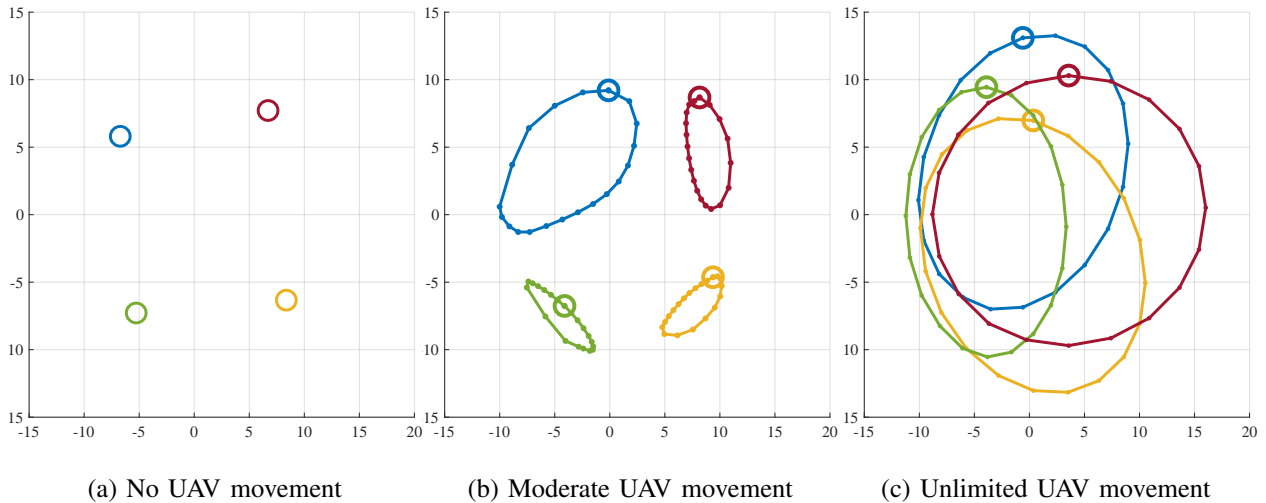


Fig. 8: Sample trajectories with 4 UAVs.

Finally, in Fig. 8, we show the optimized UAV trajectories for the three different scenarios of zero, moderate, and unlimited UAV movements. The moderate movement scenario is designed

with a Lagrange multiplier of  $\ell = \frac{3}{2}$ , and achieves the data point with a per-UAV traveled distance of approximately 21 in Fig. 7. The  $t = 0$  positions of each trajectory are marked with a circle. Each point on the trajectory corresponds to one discrete time instance that is optimized via the trajectory optimization algorithm. All UAVs travel “clockwise.”

## VII. CONCLUSIONS AND EXTENSIONS

We have studied the optimal deployment and relocation of UAV networks. We have first considered the case of variable ground terminal (GT) transmission power with fixed data rate. For static networks without any GT density variations, we have found the asymptotically optimal UAV locations that minimize the average GT power consumption. We have also provided analytical and numerical methods for dynamic UAV deployment where the GT density varies over time. In particular, we have found the asymptotically optimal UAV trajectories for one-dimensional networks and an unlimited UAV movement. We have also introduced a trajectory optimization algorithm for finding good trajectories for moderate UAV movement constraints.

Last but not least, let us also discuss the case of variable-rate fixed-power systems. In this case, each GT transmits with a fixed power  $P$ , resulting in the achievable average rate (in nats/sec/Hz)

$$R(\mathbf{x}, f) \triangleq \int_{\mathbb{R}^d} \log \left( 1 + \frac{P}{(\min_i \|x_i - q\|^2 + h^2)^{\frac{r}{2}}} \right) f(q) dq, \quad (47)$$

as the variable-rate analogue of (1). For a large number of UAVs, a Taylor expansion yields

$$R(\mathbf{x}, f) = \log \left( 1 + \frac{P}{hr} \right) - \frac{\frac{1}{2}rP/h^2}{P + hr} \int_{\mathbb{R}^d} \min_i \|x_i - q\|^2 f(q) dq + \int_{\mathbb{R}^d} o \left( \min_i \|x_i - q\|^2 \right) f(q) dq. \quad (48)$$

This final expression is in the same form as (10); the only differences are in the constants. All of our asymptotic results thus extend to variable-rate systems in a straightforward manner.

## ACKNOWLEDGEMENTS

The authors would like to thank Raheleh Khodabakhsh and Nitin Surya for their invaluable feedback on an earlier version [1] of this paper.

## APPENDIX A

## PROOF OF PROPOSITION 2

First, note that if  $g$  is monotonically increasing,  $A \subset \mathbb{R}$ , and  $x \in \mathbb{R}$ , we have  $\int_A g(\|x - q\|)dq \geq \int_B g(\|q\|)dq$ , where  $B$  is the origin-centered interval with the same measure as  $A$ . In particular, for  $g(u) = (u^2 + h^2)^{\frac{r}{2}}$ , we obtain

$$\int_A (\|x - q\|^2 + h^2)^{\frac{r}{2}} dq \geq h(\mu(A)), \quad (49)$$

where

$$h(\nu) \triangleq \int_{-\frac{1}{2}\nu}^{\frac{1}{2}\nu} (u^2 + h^2)^{\frac{r}{2}} du = 2 \int_0^{\frac{1}{2}\nu} (u^2 + h^2)^{\frac{r}{2}} du, \quad (50)$$

and  $\mu(A)$  is the Lebesgue measure of  $A$ . By differentiation, it can be shown that  $h(\nu)$  is a concave function of  $\nu$ . Now, let  $V_i \triangleq \{q : \|q - x_i\| \leq \|q - x_j\|, \forall j\}$ ,  $i = 1, \dots, n$  denote the Voronoi cells that are generated by  $x_1, \dots, x_n$ . We have

$$\begin{aligned} P(\mathbf{x}, f) &= \sum_{i=1}^n \int_{V_i} (\|x_i - q\|^2 + h^2)^{\frac{r}{2}} dq \geq \sum_{i=1}^n h(\mu(V_i)) \\ &\geq nh \left( \frac{1}{n} \sum_{i=1}^n \mu(V_i) \right) = nh \left( \frac{1}{n} \right) = 2n \int_0^{\frac{1}{2n}} (u^2 + h^2)^{\frac{r}{2}} du. \end{aligned} \quad (51)$$

The first and the second inequalities follow from (49) and the concavity of  $h(\cdot)$ , respectively. It can easily be verified that the last expression equals  $P(\mathbf{x}_u, f)$ . This concludes the proof.

## APPENDIX B

## PROOF OF LEMMA 1

Let “ $y \ll x$ ” be the shorthand notation for conditions  $\|y - u\| \leq \|x - u\|$ ,  $\|y - v\| \leq \|x - v\|$ , and  $\|y - w\| \leq \|x - w\|$ . If  $x \in T$ , we set  $y = x$ , and the proof is complete. Otherwise, let  $x_0$  be the projection of  $x$  on the two-dimensional subspace that contains  $T$ . We have  $x_0 \ll x$  by the Pythagorean inequality. If  $x_0 \in T$ , the lemma then follows with  $y = x_0$ . Otherwise, by appropriate translations of vectors  $u, v, w, x_0$ , we may assume that  $u = \begin{bmatrix} 0 \\ 0 \end{bmatrix}$ ,  $v = \begin{bmatrix} v_1 \\ 0 \end{bmatrix}$ ,  $w = \begin{bmatrix} w_1 \\ w_2 \end{bmatrix}$ , and  $x_0 = \begin{bmatrix} x_{01} \\ x_{02} \end{bmatrix}$ , where  $v_1, x_{01}, x_{02} \geq 0$ ,  $w_2 \leq 0$ , and  $w_1 \in \mathbb{R}$ . Now, let  $x_1 = \begin{bmatrix} x_{01} \\ 0 \end{bmatrix}$ . The geometry so far is illustrated in Fig. 9. It is easily verified that  $\|x_1 - u\| \leq \|x_0 - u\|$  and

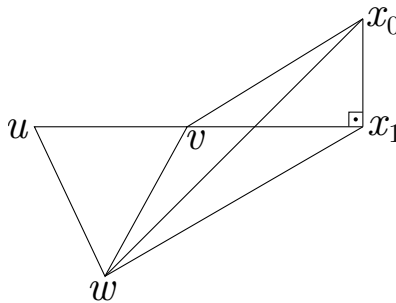


Fig. 9: The first case for the proof of Lemma 1.

$\|x_1 - v\| \leq \|x_0 - v\|$ . Also, since the angle  $\widehat{x_0x_1w}$  is at least  $90^\circ$ , we have  $\|x_1 - w\| \leq \|x_0 - w\|$ , and therefore,  $x_1 \ll x_0$ . If  $x_1 \in T$ , the lemma then holds for  $y = x_1$ . Otherwise, we consider the following three cases: The first case  $w_1 \leq v_1$  is the same scenario as illustrated in Fig. 9. In this case, we have  $v \ll x_1$ , and since  $v \in T$  obviously, the proof is complete with  $y = v$ . The second case  $v_1 \leq w_1 \leq x_{01}$  is illustrated in Fig. 10. We let  $x_2 = \begin{bmatrix} w_1 \\ 0 \end{bmatrix}$ , and  $x_3$  to be the projection of  $x_2$  on the edge  $vw$ . The relation  $x_2 \ll x_1$  obviously holds. The relation  $x_3 \ll x_2$

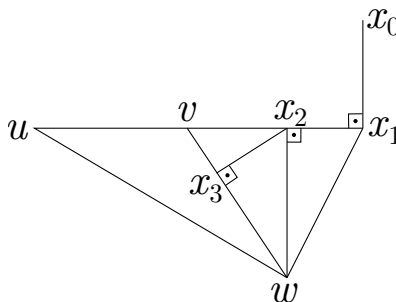


Fig. 10: The second case for the proof of Lemma 1.

follows from the same arguments that we have used to prove  $x_1 \ll x_0$  in Fig. 9. Since  $x_3 \in T$ , the lemma follows with  $y = x_3$ . Finally, for the third case  $w_1 \geq x_{01}$ , let  $x_4$  to be the projection of  $x_1$  on the edge  $vw$ . The proof of the relation  $x_4 \ll x_1$  similarly follows the proof of  $x_1 \ll x_0$  in Fig. 9. The lemma then holds for  $y = x_4$ . This concludes the proof.

## APPENDIX C

## PROOF OF PROPOSITION 5

Let  $\phi_1(x) = |x - u| + |x - v|$  and  $\phi_2(x) = c|x - w|^2$ . Without loss of generality, let  $u \leq v$ . We have  $\phi_1(x) \geq v - u$  with equality if and only if  $x \in [u, v]$ , and  $\phi_2(x) \geq 0$  with equality if and only if  $x = w$ . Therefore,  $\phi(x) \geq v - u$  with equality if and only if  $x = w$  and  $x \in [u, v]$ , or equivalently, if  $x = w$  and  $w \in [u, v]$ . This proves the first case in (41).

Suppose  $w > v$ . We first show that  $x^* \in [v, w]$ . We have  $x^* \in [u, w]$  by Lemma 1. Moreover, for any  $x \in [u, v]$ , we have  $\phi(x) = v - u + c|x - w|^2 \geq v - u + c|v - w|^2$  with equality if and only if  $x = v$ . Hence,  $x^* \in [u, v]$  implies  $x^* = v$ . Combining with  $x^* \in [u, w]$  yields  $x^* \in [v, w]$ .

Now, let  $\xi(x) = |2x - u - v| + c|x - w|^2$ . We have  $\xi(x) \leq \phi(x)$  for all  $x \in \mathbb{R}$ . Equality holds if and only if  $x \leq u$  or  $x \geq v$ . Let  $y^* = \arg \min_{x \in \mathbb{R}} \xi(x)$  denote the global minimizer of  $\xi$ . According to [40], we have

$$y^* = (w - \alpha) \in [u, w]. \quad (52)$$

If further  $y^* \in [v, w]$ , we have

$$y^* = \arg \min_{x \in [v, w]} \xi(x) = \arg \min_{x \in [v, w]} \phi(x) \quad (53)$$

$$= \arg \min_{x \in \mathbb{R}} \phi(x) = x^*. \quad (54)$$

Otherwise, if  $y^* \leq v$ , first note that  $\xi$  is increasing on  $[v, \infty)$  as  $\xi$  is convex. It follows that  $\phi$  is increasing on  $[v, \infty)$ . Since  $x^* \in [v, w]$  as already shown,  $\phi$  attains its minimum at  $x^* = v$ . Hence, we have  $x^* = \max\{v, y^*\} = \max\{v', w - \alpha\}$  in general, and this proves the second case in (41). The final case in (41) follows from the same arguments.

## REFERENCES

- [1] E. Koyuncu, R. Khodabakhsh, N. Surya, and H. Seferoglu, "Deployment and trajectory optimization for UAVs: A quantization theory approach," *IEEE Wireless Commun. Networking Conf.*, Apr. 2018.
- [2] Y. Zeng, R. Zhang, and T. J. Lim, "Wireless communications with unmanned aerial vehicles: Opportunities and challenges," *IEEE Commun. Mag.*, vol. 54, no. 5, pp. 36–42, May 2016.
- [3] I. Bor-Yaliniz and H. Yanikomeroglu, "The new frontier in RAN heterogeneity: Multi-tier drone-cells," *IEEE Commun. Mag.*, vol. 54, no. 11, pp. 48–55, Nov. 2016.

- [4] M. Mozaffari, W. Saad, M. Bennis, Y.-H. Nam, and M. Debbah, "A tutorial on UAVs for wireless networks: Applications, challenges, and open problems," Mar. 2018. [Online] Available: <https://arxiv.org/pdf/1803.00680.pdf>
- [5] R. I. Bor-Yaliniz, A. El-Keyi, and H. Yanikomeroglu, "Efficient 3-D placement of an aerial base station in next generation cellular networks," *IEEE Intl. Conf. Commun.*, May 2016.
- [6] E. Kalantari, H. Yanikomeroglu, and A. Yongacoglu, "On the number and 3D placement of drone base stations in wireless cellular networks," *IEEE Veh. Tech. Conf.*, Sept. 2016.
- [7] J. Lyu, Y. Zeng, R. Zhang, and T. J. Lim, "Placement optimization of UAV-mounted mobile base stations," *IEEE Commun. Lett.*, vol. 21, no. 3, pp. 604–607, Mar. 2017.
- [8] M. Mozaffari, W. Saad, M. Bennis, and M. Debbah, "Wireless communication using unmanned aerial vehicles (UAVs): Optimal transport theory for hover time minimization," *IEEE Trans. Wireless Commun.*, vol. 16, no. 12, pp. 8052–8066, Sept. 2017.
- [9] S. Rohde, M. Putzke, and C. Wietfeld, "Ad hoc self-healing of OFDMA networks using UAV-based relays," *Ad Hoc Nets.*, vol. 11, no. 7, Sept. 2013.
- [10] E. Koyuncu, "Power-efficient deployment of UAVs as relays," Mar. 2018. [Online] Available: <https://arxiv.org/abs/1803.04315>
- [11] M. M. Azari, Y. Murillo, O. Amin, F. Rosas, M.-S. Alouini, and S. Pollin, "Coverage maximization for a poisson field of drone cells," *IEEE Packet, Indoor and Mob. Radio Commun. Conf.*, Oct. 2017.
- [12] J.-S. Marier, C.-A. Rabbath, and N. Léchevin, "Health-aware coverage control with application to a team of small UAVs," *IEEE Trans. Control Sys. Tech.*, vol. 21, no. 5, pp. 1719–1730, Sept. 2013.
- [13] Y. Zeng and R. Zhang, "Energy-efficient UAV communication with trajectory optimization," *IEEE Trans. Wireless Commun.*, vol. 16, no. 6, pp. 3747–3760, June 2017.
- [14] K. Anazawa, P. Li, T. Miyazaki, and S. Guo, "Trajectory and data planning for mobile relay to enable efficient Internet access after disasters," *IEEE Global Commun. Conf.*, Dec. 2015.
- [15] F. Jiang and A. L. Swindlehurst, "Optimization of UAV heading for the ground-to-air uplink," *IEEE J. Select. Areas Commun.*, vol. 30, no. 5, pp. 993–1005, June 2012.
- [16] J. Gong, T.-H. Chang, C. Shen, and X. Chen, "Aviation time minimization of UAV for data collection over wireless sensor networks," *ArXiv preprint*, Jan. 2018. [Online] Available: <https://arxiv.org/abs/1801.02799>
- [17] H. Wang, G. Ren, J. Chen, G. Ding, and Y. Yang, "Unmanned aerial vehicle-aided communications: Joint transmit power and trajectory optimization," to appear in *IEEE Wireless Commun. Lett.*, Jan. 2018.
- [18] L. Liu, S. Zhang, and R. Zhang, "CoMP in the sky: UAV placement and movement optimization for multi-user communications," Feb. 2018. [Online] Available: <https://arxiv.org/pdf/1802.10371.pdf>
- [19] Y. Zeng, X. Xu, and R. Zhang, "Trajectory design for completion time minimization in UAV-enabled multicasting," to appear in *IEEE Trans. Wireless Commun.*, Jan. 2018.
- [20] M. Mozaffari, W. Saad, M. Bennis, and M. Debbah, "Mobile unmanned aerial vehicles (UAVs) for energy-efficient internet of things communications," *IEEE Trans. Wireless Commun.*, vol. 16, no. 11, pp. 7574–7589, Nov. 2017.
- [21] Y. Zeng, R. Zhang, and T. J. Lim, "Throughput maximization for UAV-enabled mobile relaying systems," *IEEE Trans.*

- Commun.*, vol. 64, no. 12, pp. 4983–4996, Dec. 2016.
- [22] P. Zhan, K. Yu, and A. L. Swindlehurst, “Wireless relay communications with unmanned aerial vehicles: Performance and optimization,” *IEEE Trans. Aerospace Elect. Syst.*, vol. 47, no. 3, pp. 2068–2085, July 2011.
- [23] D. S. Kalogerias and A. P. Petropulu, “Enhancing QoS in spatially controlled beamforming networks via distributed stochastic programming,” *IEEE Intl. Conf. Acoustics Speech Signal Process.*, Mar. 2017.
- [24] S. Zhang, H. Zhang, Q. He, K. Bian, and L. Song, “Joint trajectory and power optimization for UAV relay networks,” *IEEE Commun. Lett.*, vol. 22, no. 1, pp. 161–164, Jan. 2018.
- [25] D. H. Choi, S. H. Kim, and D. K. Sung, “Energy-efficient maneuvering and communication of a single UAV-based relay,” *IEEE Trans. Aerosp. Electron. Syst.*, vol. 50, no. 3, pp. 2320–2327, Jul. 2014.
- [26] S. Jeong, O. Simeone, and J. Kang, “Mobile edge computing via a UAV-mounted cloudlet: Optimization of bit allocation and path planning,” *IEEE Trans. Veh. Tech.*, May. 2017 (to appear).
- [27] R. M. Gray and D. L. Neuhoff, “Quantization,” *IEEE Trans. Inf. Theory*, vol. 44, no. 6, pp. 2325–2383, Oct. 1998.
- [28] A. Okabe, B. Boots, K. Sugihara, and S. N. Chiu, *Spatial Tessellations: Concepts and Applications of Voronoi Diagrams*, 2nd ed., Wiley Series in Probability and Statistics. New York, NY: John Wiley & Sons, 2000.
- [29] E. Koyuncu, “Performance gains of optimal antenna deployment in massive MIMO systems,” *IEEE Trans. Wireless Commun.*, Feb. 2018 (to appear).
- [30] Y. Song, B. Wang, Z. Shi, K. R. Pattipati, and S. Gupta, “Distributed algorithms for energy-efficient even self-deployment in mobile sensor networks,” *IEEE Trans. Mobile Comput.*, vol. 13, no. 5, pp. 1035–1047, May 2014.
- [31] E. Koyuncu and H. Jafarkhani, “On the minimum average distortion of quantizers with index-dependent distortion measures,” *IEEE Trans. Signal Process.*, vol. 65, no. 17, pp. 4655–4669, Sept. 2017.
- [32] S. P. Lloyd, “Least squares quantization in PCM,” *IEEE Trans. Inf. Theory*, vol. 28, no. 2, pp. 129–137, Mar. 1982.
- [33] Y. Linde, A. Buzo, and R. Gray, “An algorithm for vector quantizer design,” *IEEE Trans. Commun.*, vol. 28, no. 1, pp. 84–95, Jan. 1980.
- [34] J. Cortes, S. Martinez, T. Karatas, F. Bullo, “Coverage control for mobile sensor networks,” *IEEE Trans. Robot. Automat.*, vol. 20, no. 2, pp. 243–255, Apr 2004.
- [35] A. Gusrialdi, S. Hirche, T. Hatanaka, and M. Fujita, “Voronoi based coverage control with anisotropic sensors,” *American Control Conf.*, June 2008.
- [36] J. Guo and H. Jafarkhani, “Movement-efficient sensor deployment in wireless sensor networks,” *IEEE Intl. Conf. Commun.*, May 2018.
- [37] W. R. Bennett, “Spectra of quantized signals,” *The Bell System Tech. J.*, vol. 27, no. 3, pp. 446–472, July 1948.
- [38] P. L. Zador, “Asymptotic quantization error of continuous signals and the quantization dimension,” *IEEE Trans. Inf. Theory*, vol. 28, no. 2, pp. 139–148, Mar. 1982.
- [39] P. A. Chou, T. Lookabaough, and R. M. Gray, “Entropy-constrained vector quantization,” *IEEE Trans. Acoustics, Speech and Signal Process.*, vol. 37, no. 1, pp. 31–42, Jan. 1989.
- [40] p.s. (<https://math.stackexchange.com/users/17433/p-s>), “min : sum of L2 norm and squared-L2 norm,” *Mathematics Stack Exchange*, [Online] Available: <https://math.stackexchange.com/q/931702> (version: 2014-09-15).